Fluctuation-induced dispersion forces on thin DNA films

Lixin Ge,[1,*] Xi Shi,[2] Bingzhong Li,[1] and Ke Gong[1]
[1]*School of Physics and Electronic Engineering, Xinyang Normal University, Xinyang 464000, China*
[2]*Department of Physics, Shanghai Normal University, Shanghai 200234, China*

(Received 26 January 2023; revised 5 April 2023; accepted 15 May 2023; published 5 June 2023)

In this work, the calculation of Casimir forces across thin DNA films is carried out based on the Lifshitz theory. The variations of Casimir forces due to the DNA thicknesses, volume fractions of containing water, covering media, and substrates are investigated. For a DNA film suspended in air or water, the Casimir force is attractive, and its magnitude increases with decreasing thickness of DNA films and the water volume fraction. For DNA films deposited on a dielectric (silica) substrate, the Casimir force is attractive for the air environment. However, the Casimir force shows unusual features in a water environment. Under specific conditions, switching sign of the Casimir force from attractive to repulsive can be achieved by increasing the DNA-film thickness. Finally, the Casimir force for DNA films deposited on a metallic substrate is investigated. The Casimir force is dominated by the repulsive interactions at a small DNA-film thickness for both the air and water environments. In a water environment, the Casimir force turns out to be attractive for a large DNA-film thickness, and a stable Casimir equilibrium can be found. The influences of electrolyte screening on the Casimir pressure of DNA films are also discussed at the end. In addition to the adhesion stability, our finding could be applicable to the problems of condensation and decondensation of DNA, due to fluctuation-induced dispersion forces.

DOI: 10.1103/PhysRevE.107.064402

I. INTRODUCTION

The dispersion force is generated by fluctuating dipoles, resulting from the zero-point vacuum fluctuation and thermal fluctuation [1]. When the consumption time for propagating waves between the fluctuating dipoles is larger than or comparable to the lifetime of the fluctuating dipoles, the retardation effect (or wave effect) can modify the decay laws of the dispersion force [2]. Specifically, the dispersion force is known as the van der Waals force for closely spaced objects or interfaces [3], where the retardation is negligible. The retardation effect manifests when the separation distance is large, and the dispersion force is also named the retarded van der Waals force [4] or the Casimir force [5–7]. In some configurations, the retardation effect can be apparent even at a separation of several nanometers [8]. The dispersion force and its free energy play an important role in various disciplines, ranging from nanomechanics [9–13] and wetting phenomena [14–16] to ice premelting and formation [17–20], etc. In addition, the dispersion force and its free energy across organic films were also investigated intensely [7,21–26]. It was reported that the attractive dispersion force would make organic films more stable, while the repulsive force has an opposite effect [23–26].

Deoxyribonucleic acid (DNA), composed of two helical polynucleotide chains, is one of the most important macromolecules in biology. Along with its biological functions, the material properties of DNA are of great interest for the state-of-art of nanotechnology, motivated by the promising applications in a variety of fields, such as self-assembly of colloidal nanoparticles [27–30], DNA-based nanomedicines [31–34], organic nanophotonics [35,36], etc. DNA films have been widely applied as one of the crucial elements in many bio-organic nanoscale devices [37–40]. DNA films are generally deposited on inorganic substrates using the spin coating process [40]. The structure stability of double-stranded DNA is determined by the hydrogen bonds between nucleotides and the base-stacking interactions [41]. However, the adhesion stability of DNA films placed on a substrate is dependent on the surface forces [15,42], such as ionic or electrostatic forces, intrahydrogen bonds, dispersion forces, etc. The dispersion force is an important ingredient of the surface forces, particularly, when the thickness of a bio-organic film is miniaturized to a submicrometer scale [23]. Moreover, the other surface forces (e.g., intrahydrogen bonds) could be absent at the surface of some specific substrates. Then, it is expected that the contribution from the dispersion force becomes more prominent, and quantitative calculations of this force are necessary.

In this work, we study the Casimir force of DNA films within the framework of Lifshitz theory. The influences of Casimir forces due to DNA-film thicknesses, water volume fractions, background media, and substrates are investigated by numerical calculations. We find that the Casimir pressure is attractive for a DNA film suspended in air or water, and its magnitude increases by decreasing the DNA-film thickness and water volume fraction. For a DNA film placed on a silica substrate with air background, the Casimir pressure shows a trend similar to that in the suspended configuration. However, the Casimir pressure exhibits rich features when the setup is immersed in water. Under specific water volume fraction, sign switching of the Casimir pressure across a wet DNA film is

*lixinge@hotmail.com

revealed by increasing the DNA-film thickness. Finally, the Casimir pressure for a DNA film placed on a metallic substrate is also calculated. It is found that the Casimir pressure is dominated by the repulsive interactions at a small DNA-film thickness for both the air and water environments. Interestingly, a stable Casimir equilibrium is found when the DNA film is immersed in water. The electrolyte screening on the Casimir pressure of DNA films is also discussed at the end. Our findings could be applicable to the problems of adhesive stability and condensation and decondensation of DNA films, due to the fluctuation-induced dispersion forces.

II. THEORETICAL MODELS

We consider a DNA film sandwiched between a cladding medium and a substrate. The thicknesses of the cladding layer and substrate are assumed to be semi-infinite. In addition, the whole system is in thermal equilibrium at room temperature T. The Casimir pressure of the DNA film is calculated based on the framework of the Lifshitz theory [6,24]:

$$P_c(a) = -\frac{k_b T}{\pi}{\sum_{n=0}^{\infty}}' \int_0^{\infty} k_{\parallel} k_3 dk_{\parallel} \sum_{\alpha=s,p} \frac{r_1^{\alpha} r_2^{\alpha} e^{-2k_3 a}}{1 - r_1^{\alpha} r_2^{\alpha} e^{-2k_3 a}}, \quad (1)$$

where a is the thickness of the DNA film, the prime in summation denotes a prefactor $1/2$ for the term $n = 0$, k_b is Boltzmann's constant, $k_3 = \sqrt{k_{\parallel}^2 + \varepsilon_D(i\xi_n)\xi_n^2/c^2}$ is the vertical wave vector in the DNA film, $k_{\parallel}$ is the parallel wave vector, c is the speed of light in vacuum, $\varepsilon_D(i\xi_n)$ is the permittivity of the dry DNA film, $\xi_n = 2\pi \frac{k_b T}{\hbar} n$ $(n = 0, 1, 2, 3, \dots)$ are the discrete Matsubara frequencies, $\hbar$ is the reduced Planck constant, and r^{α} $(\alpha = s, p)$ are the reflection coefficients for the DNA film, where the superscripts $\alpha = s$ and p correspond to the polarizations of transverse electric (TE) and transverse magnetic (TM) modes, respectively. The subscripts 1 and 2 denote the reflection coefficients at the top and bottom interfaces of DNA film, respectively.

The reflection coefficients for an electromagnetic wave incident from the DNA film to a medium (with permittivity ε_1) are given as [24]

$$r^{\mathrm{TM}} = \frac{\varepsilon_1(i\xi_n)k_3(i\xi_n, k_{\parallel}) - \varepsilon_D(i\xi_n)k_1(i\xi_n, k_{\parallel})}{\varepsilon_1(i\xi_n)k_3(i\xi_n, k_{\parallel}) + \varepsilon_D(i\xi_n)k_1(i\xi_n, k_{\parallel})}, \quad (2)$$

$$r^{\mathrm{TE}} = \frac{k_3(i\xi_n, k_{\parallel}) - k_1(i\xi_n, k_{\parallel})}{k_3(i\xi_n, k_{\parallel}) + k_1(i\xi_n, k_{\parallel})}, \quad (3)$$

where $k_1 = \sqrt{k_{\parallel}^2 + \varepsilon_1(i\xi_n)\xi_n^2/c^2}$ is the vertical wave vector in medium 1. Here, medium 1 can be air, water, silica, or gold.

The reflection coefficients are strongly dependent on the permittivity at different Matsubara frequencies. Here, the dielectric functions of used materials are fitted by a model of the modified harmonic oscillator, which is adopted from recent literature [43]:

$$\varepsilon(i\xi) = 1 + \sum_j \frac{C_j}{1 + (\xi/\omega_j)^{\beta_j}}, \quad (4)$$

where C_j corresponds to the oscillator strength for the jth resonance frequency ω_j, and β_j is a power exponent. In addition to the Kramers-Kronig relations, the influences of the electronic dielectric constant, optical bandgap, density, and chemical composition are taken into account in Eq. (4), where the parameters for the dry DNA, water, and silica are shown in Table I.

TABLE I. The parameters for the used materials [43].

	C_j	ω_j (eV)	β_j
		DNA	
$j = 1$	1.766	0.0056	1.03
$j = 2$	1.431	12.95	1.67
		Water	
$j = 1$	73.48	8.1×10^{-5}	0.988
$j = 2$	2.534	0.016	1.1
$j = 3$	0.755	16.1	1.751
		Silica	
$j = 1$	1.843	0.0725	1.678
$j = 2$	1.105	15.33	1.71

Specifically, the dielectric responses of DNA are also dependent on the composition and stacking sequence [44]. Here, the DNA is assumed to have one cytosine, one guanine, one adenine, one thymine, four sugar groups and four phosphate groups. Hence, the molecular formula of DNA is written as $C_{39}H_{45}N_{15}O_{24}P_4$. It is worth mentioning that the dielectric function of the dry DNA given by the parameters in Table I matches the measured data of DNA over a wide range of frequencies, from zero frequency to the far ultraviolet [43,45–48]. Based on the Clausius-Mossotti equation, the permittivity for a wet DNA (denoted by ε_D') is given by the following form [14,23]:

$$\frac{\varepsilon_D'(i\xi_n) - 1}{\varepsilon_D'(i\xi_n) + 2} = \Phi \frac{\varepsilon_w(i\xi_n) - 1}{\varepsilon_w(i\xi_n) + 2} + (1 - \Phi)\frac{\varepsilon_D(i\xi_n) - 1}{\varepsilon_D(i\xi_n) + 2}, \quad (5)$$

where $\varepsilon_w(i\xi_n)$ is the permittivity of water and Φ is the volume fraction of water in the DNA film.

The dielectric function of gold is given by summing up the Drude model and the modified harmonic oscillator, which is written as [43]

$$\varepsilon(i\xi) = 1 + \frac{C_1}{1 + (\xi/\omega_1)^{\beta_1}} + \frac{\omega_p^2}{\xi^2 + \gamma\xi}, \quad (6)$$

where the parameters $C_1 = 6.5$, $\omega_1 = 5.9$ (eV), $\beta_1 = 1.42$, $\omega_p = 9.1$ (eV), and $\gamma = 0.06$ (eV). We find that the Casimir calculations based on the gold permittivity in the Eq. (6) are the same as those given by the generalized Drude-Lorentz model [49].

III. RESULTS AND DISCUSSIONS

Figure 1(a) shows the permittivity of the applied materials evaluated in imaginary frequency. The results show that the permittivity of dry DNA is larger than those of water and silica for the Matsubara term $n > 0$. The permittivity of water is the smallest over a wide range of frequencies. Figure 1(b) shows the permittivity of DNA under different water volume fractions. As expected, the permittivity of wet DNA decreases by increasing the magnitude of Φ, due to the elevated contribution from the low-refractive-index water.

To predict the sign of Casimir pressure, the permittivity at $n = 0$ is significant since it plays a dominant role at large

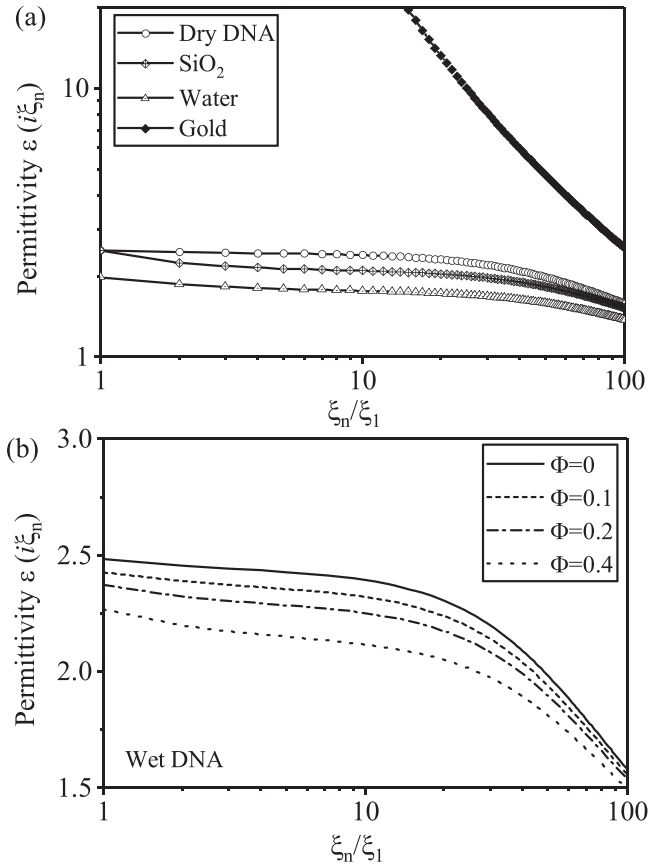

FIG. 1. (a) The permittivity of used materials evaluated in imaginary frequency. (b) The permittivity of wet DNA containing different volume fractions of water.

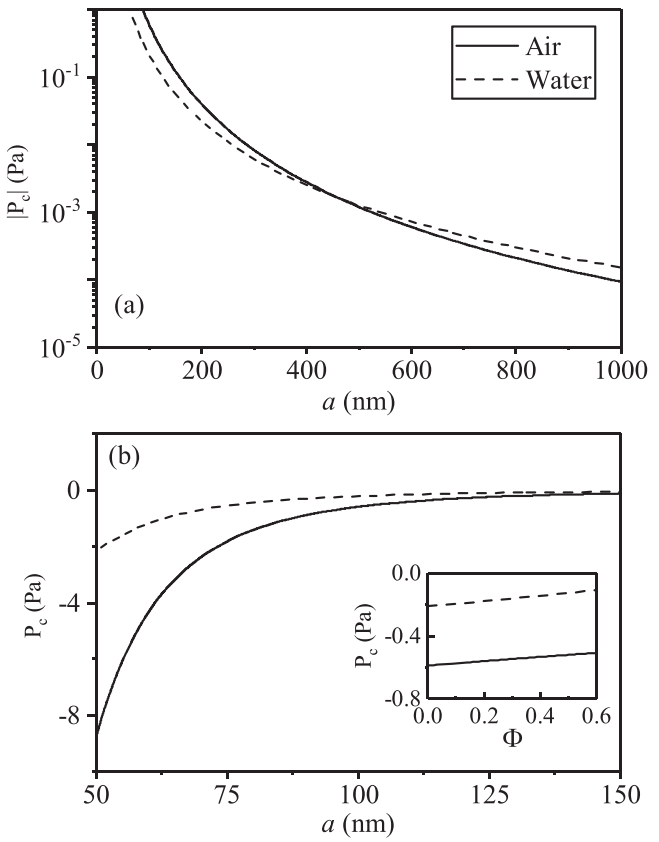

FIG. 2. (a) The magnitude of Casimir pressure versus the thickness of a dry DNA film suspended in backgrounds of air and water. (b) The Casimir pressure for thinner DNA films on a linear scale. The inset shows the Casimir pressure as a function of water volume fraction, where the DNA-film thickness $a = 100$ nm is fixed. The temperature is 300 K.

thickness (or separation), as reported in [23,50]. The static permittivities for the silica, DNA, and water are about 3.9, 4.2, and 81, respectively. However, the dielectric function of a wet DNA film at $n = 0$ shows a different trend, compared with the high-frequency one. The static permittivity $\varepsilon'_{\rm D}$ increases from 4.2 to 11.9, with increasing Φ from 0 to 0.6.

A. The Casimir pressures for suspended DNA films

We first consider the Casimir force of a DNA film suspended in a homogeneous background medium. The Casimir force would be attractive as reported for suspended peptide films [24]. The absolute Casimir pressure versus the thickness of suspended DNA film is shown in Fig. 2(a), where the solid and dashed lines represent the background media of air and water, respectively. It is found that the magnitude of Casimir pressure decreases monotonically by increasing the DNA thickness. The Casimir pressure in air is larger than that in water at a small thickness, while it is smaller at a larger thickness.

The sign and magnitude of the Casimir pressure are dependent on the dielectric responses of materials. Considering the cases of DNA film surrounded by medium 1 and medium 2, the Casimir pressure would be proportional to the permittivity contrasts of the media [51],

$$P_c \propto \left(\frac{\varepsilon_1(i\xi)-\varepsilon_{\rm D}(i\xi)}{\varepsilon_1(i\xi)+\varepsilon_{\rm D}(i\xi)}\right)\left(\frac{\varepsilon_2(i\xi)-\varepsilon_{\rm D}(i\xi)}{\varepsilon_2(i\xi)+\varepsilon_{\rm D}(i\xi)}\right), \qquad (7)$$

where ε_1 and ε_2 are the permittivities of medium 1 and medium 2, respectively. We have $\varepsilon_1(i\xi) = \varepsilon_2(i\xi) = 1$, $\varepsilon_1(i\xi) = \varepsilon_2(i\xi) = \varepsilon_{\rm w}(i\xi)$ when the DNA film is suspended in air and water, respectively. The permittivity contrasts between DNA film and air are larger than those of water for $n > 0$. It is known that the high frequency components are dominant for the calculation of Casimir force at a small separation [52]. As a result, the Casimir pressure for air is larger than that of water at a small DNA thickness. By contrast, the dielectric contrast between DNA film and water is much larger than that of air at $n = 0$, which is the leading term for a large DNA-film thickness. Thus, there is no surprise that the Casimir pressure in a water environment is larger than that with the configuration of air for a large thickness (e.g., $a > 500$ nm).

On the other hand, it would be interesting to consider the Casimir pressure across a wet DNA film. As an example, we set the thickness $a = 100$ nm, and the Casimir force versus the volume fraction of water in DNA film is shown in the inset of Fig. 2(b). The results show that the magnitude increases

with decreasing the value of Φ. At the limit $\Phi = 0$, the attractive Casimir pressures in the air and water environments are about 0.2 and 0.6 Pa, respectively. The magnitude of Casimir pressure is hundreds of times larger than the gravity of the DNA film (about 1.7 mPa for $a = 100$ nm), manifesting the important role of the fluctuation-induced force. It can be seen that the magnitude of Casimir pressure can be enlarged over 10 times, when the thickness a decreases further from 100 to 50 nm.

Interestingly, the trends of Casimir pressure versus the water volume fraction are opposite between the thin DNA and peptide films [24]. These discrepancies are attributed to the frequency-dependent dielectric permittivities of DNA, peptide, and water. Considering a wet DNA (peptide) film with a fixed thickness of 100 nm suspended in air, the leading contributions to the Casimir pressure are the terms $n \geqslant 1$. At these frequencies, the permittivity $\varepsilon(i\xi_n)$ of the DNA (peptide) film is larger (smaller) than that of water. Hence, the permittivity of the wet DNA film would decrease with increasing Φ. By contrast, the permittivity of the wet peptide film increases with increasing Φ, resulting in an opposite trend of Casimir pressure.

Note that the condensation of DNA will decrease its thickness and the volume fraction of water (i.e., squeezing the water out of the DNA film). Hence, it can be concluded that DNA films trends toward condensation for suspended configurations, due to the attractive Casimir force.

B. The Casimir pressures for a silica substrate

In many organic devices, the DNA film is generally deposited on a dielectric substrate. The Casimir pressure for a DNA thin film placed on a silica substrate is shown in Fig. 3(a), where the cladding background medium is air. The result shows that the Casimir pressure is negative, and its magnitude increases by decreasing the DNA-film thickness. We note that the magnitude of the Casimir pressure is about 0.07 Pa for the dry DNA film at 100 nm, which declines considerably compared with the suspended configuration (about 0.6 Pa). In addition, the magnitude of the Casimir pressure for wet DNA film declines further with increasing volume fraction Φ. The pressure is only about 0.04 Pa with volume fraction $\Phi = 0.4$. Nonetheless, the Casimir pressure for wet DNA deposited on a silica substrate is still much larger than the gravity of the DNA film. Overall, a thin DNA film and a low water volume fraction are preferred for stability of the DNA film.

We find that the Casimir properties for DNA film deposited on silica are quite different from the case of peptide films [53]. It is suggested that the sign of the Casimir pressure can change from negative to positive when the peptide-film thickness decreases below a critical value (ranging from 115 to 133 nm), depending on the fraction of water in the peptide film [53]. These discrepancies are attributed to the different dielectric responses of DNA, peptide, and silica. The permittivity $\varepsilon(i\xi_n)$ of dry DNA (peptide) is larger (smaller) than that of silica over a vast range of frequency ($n \geqslant 0$). When the films are wetted by water, the static permittivity $\varepsilon(i\xi_{n=0})$ of peptide becomes larger than that of silica, reversing the sign of the Casimir pressure at a specific film thickness. On the other hand, the permittivity of a wet DNA film is larger than those of silica and air over a vast range of frequencies, resulting in a negative Casimir pressure for thin films in Fig. 3(a).

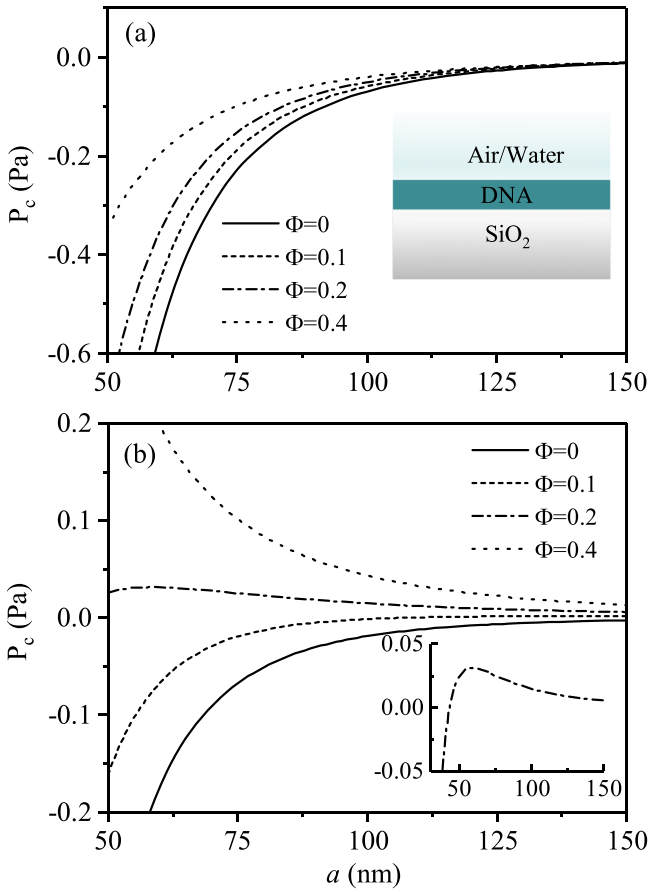

FIG. 3. The Casimir pressure versus the thickness of DNA films under different volume fractions Φ. The substrate consists of semi-infinite silica. (a) The DNA film is exposed to air. (b) The DNA film is immersed in water. The inset in (b) shows the Casimir pressure for $\Phi = 0.2$ with a clearer plot scale. The positive (negative) sign of the pressure corresponds to the repulsive (attractive) force.

As the DNA film is immersed in water, some complicated or even reverse conclusions are obtained, in comparison with the air configurations. The Casimir pressure as a function of the thickness a is shown in Fig. 3(b). The results show that the Casimir pressure is long-range negative at low volume fractions 0 and 0.1, and its magnitude decreases rapidly with increasing DNA-film thickness. These properties suggest that a thin DNA film is favored for stability due to the attractive Casimir force, similar to the case of air in Fig. 3(a). However, the Casimir pressure for large Φ shows different features. For $\Phi = 0.4$, the Casimir pressure is long-range positive, which means that a small thickness is harmful to the stability of DNA films. For an intermediate value $\Phi = 0.2$, the Casimir pressure turns from negative to positive with increasing thickness a, as shown in the inset of Fig. 3(b). Then, a maximum peak for the Casimir repulsion can be found near 60 nm, which contributes negatively to the stability. The Casimir pressure would decrease with further increase of the thickness a.

The unusual behavior of Casimir pressure in the water background can be interpreted by the competition between the attractive and repulsive Casimir components. For a small Φ, the permittivity of the wet DNA is larger than those of silica and water over a wide range of frequencies ($n > 0$). The dielectric permittivity of the DNA and silica are very close at zero frequency, resulting in a negligible contribution from the term $n = 0$. Therefore, the Casimir pressure is attractive according to Eq. (7), and its magnitude increases rapidly with decreasing DNA-film thickness, as demonstrated with $\Phi = 0$ and 0.1 in Fig. 3(b). For a large $\Phi = 0.4$, the permittivity of the wet DNA is smaller (larger) than that of silica (water) for $n > 0$, resulting in repulsive Casimir force. At static frequency with $n = 0$, the permittivity of the wet DNA is larger (smaller) than that of silica (water), which also leads to repulsive Casimir force. Hence, the Casimir pressure would be long-range repulsive for a large Φ. For an intermediate $\Phi = 0.2$, the permittivity of the wet DNA is still larger than that of silica (water) for $n > 0$, resulting in attractive Casimir force at a small thickness a. However, the contribution for $n = 0$ is still positive, resulting in repulsive Casimir force at a large value of a. Due to the competition between the attractive and repulsive Casimir components, the peak for Casimir repulsion is expected at an intermediate thickness, as shown in the inset of Fig. 3(b).

C. The Casimir pressures for a metallic substrate

Now we consider the case of DNA films deposited on the metallic substrate. The Casimir pressure as a function of thickness a is shown in Fig. 4(a), where the cladding medium is air. According to Eq. (7), we can predict that the Casimir pressure is long-range repulsive because $\varepsilon_{\rm air} < \varepsilon'_{\rm D} < \varepsilon_{\rm Au}$ is satisfied for $n \geqslant 0$ (see, e.g., Ref. [54]). The magnitude of Casimir pressure decreases monotonically with increasing DNA-film thickness, and this phenomenon was also found for peptide films deposited on an Au substrate [25,55]. As a result, the dispersion forces make the DNA film less stable for small thickness. Note that the discrepancy of Casimir pressures acting on the DNA film is small between volume fractions $\Phi = 0$ and 0.4.

The Casimir pressure acting on the DNA film immersed in water exhibits different characteristics, shown in Fig. 4(b). The Casimir pressure is repulsive at a small thickness, while it becomes attractive for a large thickness. At a specific thickness, a stable Casimir equilibrium, i.e., the pressure equals zero, is found. The critical thickness for the Casimir equilibrium can be modulated by the magnitude of Φ. As Φ increases from 0 to 0.4, the critical thickness decreases correspondingly from about 237 to 174 nm. The interesting Casimir equilibrium in the water background can be understood by the contrast of permittivity in Eq. (7). The repulsive relation $\varepsilon_{\rm w} < \varepsilon'_{\rm D} < \varepsilon_{\rm Au}$ is satisfied for $n > 0$, and the permittivity contrast between the water and wet DNA decreases with increasing Φ, resulting in a smaller Casimir repulsion. On the other hand, the attractive Casimir interaction for a large thickness a is attributed to the relation $\varepsilon_{\rm w} > \varepsilon'_{\rm D}$ at the leading term $n = 0$. In addition to the reversal of dielectric contrast at low and high Matsubara frequencies, the nonmonotonic Casimir pressure is also attributed to the retardation effect, which resembles the problem of the surface melting of ice [56,57].

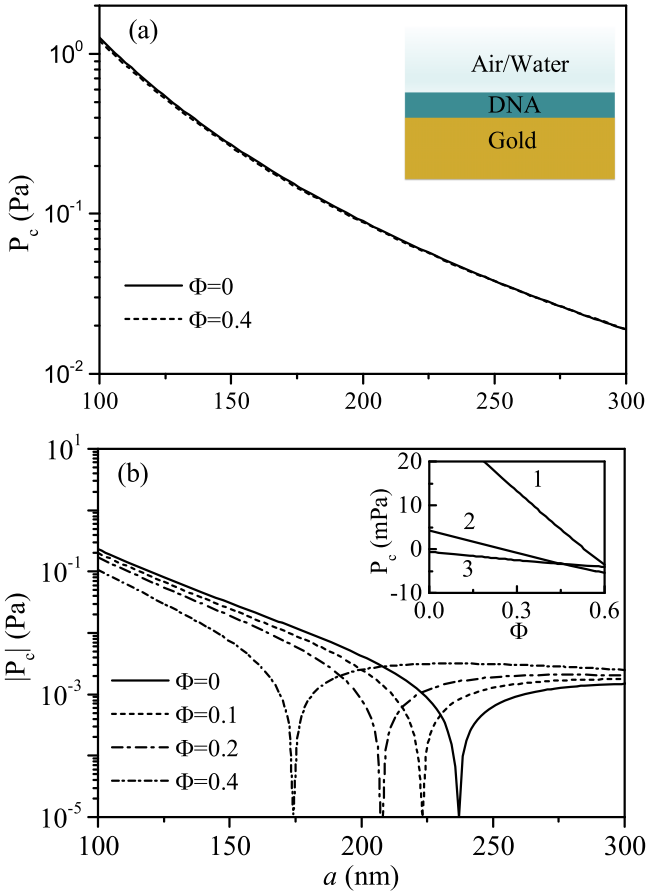

FIG. 4. The Casimir pressure versus the thickness of DNA films with a gold substrate. (a) The DNA film is exposed in air for $\Phi = 0$ (solid) and 0.4 (dashed). (b) The DNA film is immersed in water. The inset shows the corresponding Casimir pressure as a function of Φ. The labels 1, 2, and 3 represent the thicknesses of DNA film of 150, 200, and 250 nm, respectively.

The inset in Fig. 4(b) shows the Casimir pressure changed by the volume fraction of water with a fixed DNA-film thickness. We find that switching the sign of the Casimir pressure from positive to negative is achieved by increasing the volume fraction Φ for thicknesses 150 nm and 200 nm. For thickness 250 nm, the Casimir pressure is negative and its magnitude increases by increasing the volume fraction Φ. Hence, the DNA film deposited on the metallic substrate tends toward decondensation in the water environment, according to the properties of its dispersion force.

IV. ELECTROLYTE SCREENING ON THE CASIMIR PRESSURE

Water is considered as a dielectric medium for the above discussions. However, water is an electrolyte solution in a realistic system, and the effect of electrolyte screening should be taken into account [7]. Due to the ionic-charge fluctuations, the presence of salt ions in water (e.g., H^+, OH^-, Na^+, etc.) can modify the $n = 0$ Matsubara term. When the wet DNA film (labeled 3) is sandwiched between medium 1 and medium

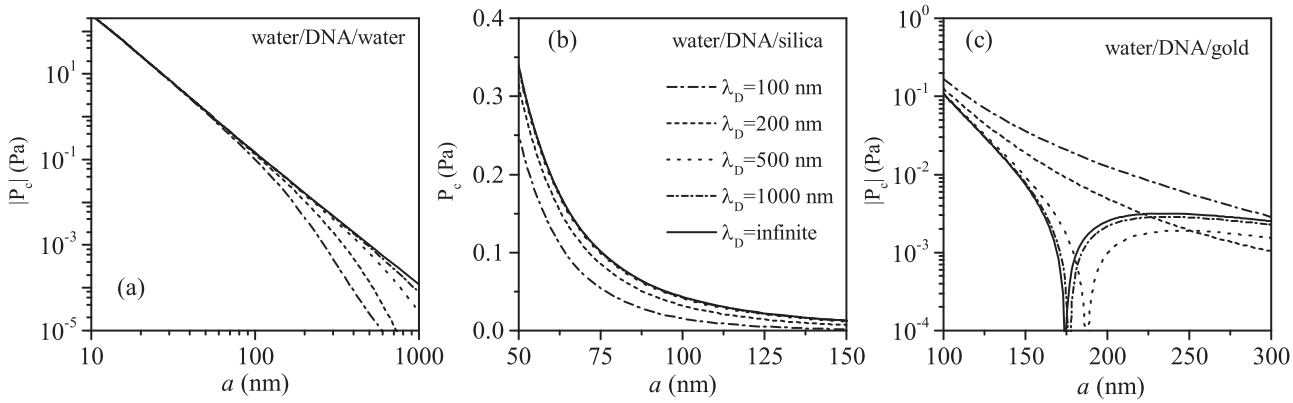

FIG. 5. The Casimir pressure versus the thickness of DNA films under different Debye lengths of water. (a) The DNA film is suspended in water. (b) The DNA film deposited on the silica substrate is immersed in water. (c) The DNA film deposited on the Au substrate is immersed in water. The water volume fraction in DNA films is set to be 0.4.

2, the Casimir pressure for the term $n = 0$ turns out to be [3]

$$P_c|_{n=0} = -\frac{k_b T}{2\pi}\int_0^\infty k_\parallel \widehat{k}_3 dk_\parallel \frac{\widehat{\Delta}_{13}\widehat{\Delta}_{23}e^{-2a\widehat{k}_3}}{1-\widehat{\Delta}_{13}\widehat{\Delta}_{23}e^{-2a\widehat{k}_3}}, \quad (8)$$

where $\widehat{k}_3 = \sqrt{k_\parallel^2 + \kappa_3^2}$, and we have

$$\widehat{\Delta}_{13} = \frac{\varepsilon_1\sqrt{k_\parallel^2+\kappa_1^2} - \varepsilon_3\sqrt{k_\parallel^2+\kappa_3^2}}{\varepsilon_1\sqrt{k_\parallel^2+\kappa_1^2} + \varepsilon_3\sqrt{k_\parallel^2+\kappa_3^2}}, \quad (9)$$

$$\widehat{\Delta}_{23} = \frac{\varepsilon_2\sqrt{k_\parallel^2+\kappa_2^2} - \varepsilon_3\sqrt{k_\parallel^2+\kappa_3^2}}{\varepsilon_2\sqrt{k_\parallel^2+\kappa_2^2} + \varepsilon_3\sqrt{k_\parallel^2+\kappa_3^2}}, \quad (10)$$

where the wave vector $\kappa_i = 1/\lambda_{D_i}$ $(i = 1, 2, 3)$, and λ_{D_i} is the Debye length in the ith electrolyte medium [3]. The Debye length is dependent on the concentration of the ions, temperature, the permittivity of the solution, etc. For pure water, the Debye length is about 1000 nm at room temperature, resulting from the ions of H^+ and OH^-. The Debye length decreases with increasing concentration of the ions in water. For instance, the Debye length of water decreases from 1000 nm to around 220 nm when the CO_2 from air dissolves into water (pH around 5.7) [58]. The Debye length is about 96 nm as the concentration of NaCl is about 10 μM in the water [59].

Figure 5(a) shows the Casimir pressure for a suspended DNA film in a water environment when the electrolyte screening is taken into account. As an example, we set the water volume fraction $\Phi = 0.4$, and simply let the Debye lengths for the wet DNA film and the surrounding water be equal (i.e., the salt concentration is the same). Our results indicate that the electrolyte screening has a negligible influence on the Casimir pressure, when the condition $a \ll \lambda_D$ is satisfied. In other words, the electrolyte screen can be neglected for a thin DNA film thickness in a low salt water. However, as the DNA-film thickness is comparable to or even larger the λ_D, the strong modulation of the Casimir pressure is revealed due to the screening effect. The magnitude of the Casimir pressure is reduced rapidly, owing to the screening of the $n = 0$ term.

For a wet DNA film deposited on a silica substrate, the modulation of the Casimir pressure due to the electrolyte screening is shown in Fig. 5(b). The silica substrate is a non-ion medium. Again, we find that the change of the Casimir pressure is small when the Debye length is much larger than the DNA film thickness. For a fixed DNA film thickness, the Casimir pressure decreases as λ_D drops from 1000 to 100 nm. When the silica substrate is replaced by gold, the corresponding Casimir pressure is shown in Fig. 5(c). We find that the Casimir equilibrium is shifted when the Debye length is reduced from 1000 to 500 nm. When λ_D decreases to 200 and 100 nm, the Casimir equilibrium is absent, and the monotonic Casimir interaction is obtained. One way to avoid the electrolyte screening is by replacing the water with some nonelectrolyte solutions.

V. CONCLUSIONS

In summary, the Casimir pressure of a DNA film is calculated in several configurations based on the Lifshitz theory. The Casimir pressure is attractive when a DNA film is suspended in air or water, and its magnitude increases with decreasing thickness of DNA film or/and the water volume fraction. Hence, the suspended DNA film trends toward condensation due to the Casimir force. The Casimir pressure is hundreds of times larger than the gravity of the DNA film for a moderate thickness (e.g., 100 nm), manifesting the important role of the fluctuation-induced interactions. For DNA films deposited on the silica substrate, the Casimir pressure is attractive for the air background. Also, a thin DNA film and a low water fraction are favored for stability. Instead, the Casimir pressure shows rich features in a water background. The Casimir pressure can be changed from attractive to repulsive by increasing the DNA-film thickness and the water fraction. Lastly, the Casimir force of a DNA film deposited on a metallic substrate is explored. The Casimir pressure is dominated by the repulsive interactions at small DNA-film thickness for both the air and water environments. For the setup immersed in a water environment, the Casimir pressure turns out to be attractive at a large DNA-film thickness, and a stable Casimir equilibrium can be found at a specific

thickness. The presence of salt ions in water can screen the $n = 0$ Matsubara term, and the effect of electrolyte screening on the Casimir pressure was discussed.

The Casimir pressure of thin DNA films shows interesting properties owing to its high refractive index, compared with peptides, silica, and water. As a result, better material data (or models) for DNA films may alter the results of numerical calculations, but should not invalidate the qualitative features in this work. For instance, the DNA film is considered to be an isotropic medium (molecules with disorder orientations) in this work, while the DNA molecules could show different mesophases in water [60,61]. Therefore, the permittivity of a DNA-film sample may change from isotropic to anisotropic, depending on the fabrication techniques. The Casimir pressures due to different morphologies of DNA films would be one of the interesting directions in future works.

ACKNOWLEDGMENTS

This work is supported by the National Natural Science Foundation of China (Grant No. 11804288 and No. 61974127), the Natural Science Foundation of Henan Province (Grant No. 232300420120), and the Shanghai Pujiang Program (21PJ1411400). The research of L.X.G. is further supported by the Nanhu Scholars Program for Young Scholars of XYNU.

[1] G. Feinberg, J. Sucher, and C.-K. Au, Phys. Rep. **180**, 83 (1989).
[2] A. W. Rodriguez, F. Capasso, and S. G. Johnson, Nat. Photonics **5**, 211 (2011).
[3] V. A. Parsegian, *Van der Waals Forces: A Handbook for Biologists, Chemists, Engineers, and Physicists* (Cambridge University Press, University, 2005).
[4] R. R. Dagastine, D. C. Prieve, and L. R. White, J. Colloid Interface Sci. **249**, 78 (2002).
[5] M. Bordag, G. L. Klimchitskaya, U. Mohideen, and V. M. Mostepanenko, *Advances in the Casimir Effect*, International Series of Monographs on Physics Vol. 145 (OUP, Oxford, 2009).
[6] G. L. Klimchitskaya, U. Mohideen, and V. M. Mostepanenko, Rev. Mod. Phys. **81**, 1827 (2009).
[7] L. M. Woods, D. A. R. Dalvit, A. Tkatchenko, P. Rodriguez-Lopez, A. W. Rodriguez, and R. Podgornik, Rev. Mod. Phys. **88**, 045003 (2016).
[8] S.-w. Lee and W. M. Sigmund, J. Colloid Interface Sci. **243**, 365 (2001).
[9] T. Gong, M. R. Corrado, A. R. Mahbub, C. Shelden, and J. N. Munday, Nanophotonics **10**, 523 (2020).
[10] D. A. Somers, J. L. Garrett, K. J. Palm, and J. N. Munday, Nature (London) **564**, 386 (2018).
[11] L. Ge, X. Shi, L. Liu, and K. Gong, Phys. Rev. B **102**, 075428 (2020).
[12] B. Munkhbat, A. Canales, B. Küçüköz, D. G. Baranov, and T. O. Shegai, Nature (London) **597**, 214 (2021).
[13] V. Esteso, S. Carretero-Palacios, and H. Míguez, J. Phys. Chem. C **119**, 5663 (2015).
[14] D. B. Hough and L. R. White, Adv. Colloid Interface Sci. **14**, 3 (1980).
[15] L. Boinovich and A. Emelyanenko, Adv. Colloid Interface Sci. **165**, 60 (2011).
[16] A. Squarcini, J. M. Romero-Enrique, and A. O. Parry, Phys. Rev. Lett. **128**, 195701 (2022).
[17] Y. Li, K. A. Milton, I. Brevik, O. I. Malyi, P. Thiyam, C. Persson, D. F. Parsons, and M. Boström, Phys. Rev. B **105**, 014203 (2022).
[18] J. Luengo-Márquez and L. G. MacDowell, J. Colloid Interface Sci. **590**, 527 (2021).
[19] V. Esteso, S. Carretero-Palacios, L. G. MacDowell, J. Fiedler, D. F. Parsons, F. Spallek, H. Míguez, C. Persson, S. Y. Buhmann, I. Brevik *et al.*, Phys. Chem. Chem. Phys. **22**, 11362 (2020).
[20] J. Fiedler, M. Boström, C. Persson, I. Brevik, R. Corkery, S. Y. Buhmann, and D. F. Parsons, J. Phys. Chem. B **124**, 3103 (2020).
[21] B.-S. Lu and R. Podgornik, Phys. Rev. E **92**, 022112 (2015).
[22] R. Blackwell, A. Hemmerle, A. Baer, M. Späth, W. Peukert, D. Parsons, K. Sengupta, and A.-S. Smith, J. Colloid Interface Sci. **598**, 464 (2021).
[23] M. A. Baranov, G. L. Klimchitskaya, V. M. Mostepanenko, and E. N. Velichko, Phys. Rev. E **99**, 022410 (2019).
[24] G. L. Klimchitskaya, V. M. Mostepanenko, and E. N. Velichko, Phys. Rev. B **102**, 161405(R) (2020).
[25] G. L. Klimchitskaya, V. M. Mostepanenko, and E. N. Velichko, Phys. Rev. B **103**, 245421 (2021).
[26] G. L. Klimchitskaya, V. M. Mostepanenko, and O. Y. Tsybin, Symmetry **14**, 2196 (2022).
[27] D. Nykypanchuk, M. M. Maye, D. Van Der Lelie, and O. Gang, Nature (London) **451**, 549 (2008).
[28] L. Y. Chou, K. Zagorovsky, and W. C. Chan, Nat. Nanotechnol. **9**, 148 (2014).
[29] W. B. Rogers, W. M. Shih, and V. N. Manoharan, Nat. Rev. Mater. **1**, 1 (2016).
[30] F. Cui, S. Marbach, J. A. Zheng, M. Holmes-Cerfon, and D. J. Pine, Nat. Commun. **13**, 2304 (2022).
[31] M. J. Campolongo, S. J. Tan, J. Xu, and D. Luo, Adv. Drug Deliv. Rev. **62**, 606 (2010).
[32] Q. Hu, H. Li, L. Wang, H. Gu, and C. Fan, Chem. Rev. **119**, 6459 (2019).
[33] J. Weiden and M. M. Bastings, Curr. Opin. Colloid Interface Sci. **52**, 101411 (2021).
[34] W. Gu, F. Meng, R. Haag, and Z. Zhong, J. Control. Release **329**, 676 (2021).
[35] A. J. Steckl, Nat. Photonics **1**, 3 (2007).
[36] H. Bui, S. A. Díaz, J. Fontana, M. Chiriboga, R. Veneziano, and I. L. Medintz, Adv. Opt. Mater. **7**, 1900562 (2019).
[37] Y. Kawabe, L. Wang, S. Horinouchi, and N. Ogata, Adv. Mater. **12**, 1281 (2000).
[38] Y. Zhang, P. Zalar, C. Kim, S. Collins, G. C. Bazan, and T.-Q. Nguyen, Adv. Mater. **24**, 4255 (2012).
[39] R. Khazaeinezhad, S. Hosseinzadeh Kassani, B. Paulson, H. Jeong, J. Gwak, F. Rotermund, D.-I. Yeom, and K. Oh, Sci. Rep. **7**, 41480 (2017).

[40] W. Jung, H. Jun, S. Hong, B. Paulson, Y. S. Nam, and K. Oh, Opt. Mater. Express **7**, 3796 (2017).
[41] P. Yakovchuk, E. Protozanova, and M. D. Frank-Kamenetskii, Nucleic Acids Res. **34**, 564 (2006).
[42] R. H. French, V. A. Parsegian, R. Podgornik, R. F. Rajter, A. Jagota, J. Luo, D. Asthagiri, M. K. Chaudhury, Y. M. Chiang, S. Granick, S. Kalinin, M. Kardar, R. Kjellander, D. C. Langreth, J. Lewis, S. Lustig, D. Wesolowski, J. S. Wettlaufer, W. Y. Ching, M. Finnis, F. Houlihan *et al.*, Rev. Mod. Phys. **82**, 1887 (2010).
[43] M. Moazzami Gudarzi and S. H. Aboutalebi, Sci. Adv. **7**, eabg2272 (2021).
[44] J. B. Schimelman, D. M. Dryden, L. Poudel, K. E. Krawiec, Y. Ma, R. Podgornik, V. A. Parsegian, L. K. Denoyer, W.-Y. Ching, and N. F. Steinmetz, Phys. Chem. Chem. Phys. **17**, 4589 (2015).
[45] A. Wittlin, L. Genzel, F. Kremer, S. Häseler, A. Poglitsch, and A. Rupprecht, Phys. Rev. A **34**, 493 (1986).
[46] T. Inagaki, R. Hamm, E. Arakawa, and L. Painter, J. Chem. Phys. **61**, 4246 (1974).
[47] T. Weidlich, S. M. Lindsay, and A. Rupprecht, Biopolymers **26**, 439 (1987).
[48] B. Paulson, I. Shin, H. Jeong, B. Kong, R. Khazaeinezhad, S. R. Dugasani, W. Jung, B. Joo, H.-Y. Lee, S. Park *et al.*, Sci. Rep. **8**, 1 (2018).
[49] L. Ge, X. Shi, Z. Xu, and K. Gong, Phys. Rev. B **101**, 104107 (2020).
[50] V. Esteso, S. Carretero-Palacios, and H. Míguez, J. Appl. Phys. **119**, 144301 (2016).
[51] I. E. Dzyaloshinskii, E. M. Lifshitz, and L. P. Pitaevskii, Adv. Phys. **10**, 165 (1961).
[52] Y. Yang, R. Zeng, H. Chen, S. Zhu, and M. S. Zubairy, Phys. Rev. A **81**, 022114 (2010).
[53] E. N. Velichko, M. A. Baranov, and V. M. Mostepanenko, Mod. Phys. Lett. A **35**, 2040020 (2020).
[54] J. N. Munday, F. Capasso, and V. A. Parsegian, Nature (London) **457**, 170 (2009).
[55] V. M. Mostepanenko, E. N. Velichko, and M. A. Baranov, J. Electron. Sci. Technol. **18**, 100023 (2020).
[56] M. Elbaum and M. Schick, Phys. Rev. Lett. **66**, 1713 (1991).
[57] J. G. Dash, A. W. Rempel, and J. S. Wettlaufer, Rev. Mod. Phys. **78**, 695 (2006).
[58] Y. Wang, S. Narayanan, and W. Wu, ACS Nano **11**, 8421 (2017).
[59] A. M. Smith, A. A. Lee, and S. Perkin, J. Phys. Chem. Lett. **7**, 2157 (2016).
[60] R. Podgornik, M. A. Aksoyoglu, S. Yasar, D. Svensek, and V. A. Parsegian, J. Phys. Chem. B **120**, 6051 (2016).
[61] F. Livolant and A. Leforestier, Prog. Polym. Sci. **21**, 1115 (1996).